Targeting of 3′-Azido 3′-Deoxythymidine (AZT)-Loaded Poly(Isohexylcyanoacrylate) Nanospheres to the Gastrointestinal Mucosa and Associated Lymphoid Tissues

Assia Dembri,[1] Marie-Jeanne Montisci,[1] Jean Charles Gantier,[1] Hélène Chacun,[1] and Gilles Ponchel[1,2]

Received December 14, 2000; accepted January 8, 2001

Purpose. The aim of the study was to evaluate the capacity of poly(isohexylcyanoacrylate) nanospheres to concentrate 3′-azido 3′-deoxythymidine (AZT) in the intestinal epithelium and associated immunocompetent cells, which are known to be one of the major reservoirs of the human immunodeficiency virus (HIV).

Methods. The tissue concentration of ^{3}H-radiolabeled AZT in the gastrointestinal (GI) tract was obtained 30 and 90 minutes after intragastric administration to rats at a dose of 0.25 mg AZT/100 g of body weight. The distribution along the intestine was determined. AZT concentrations in the lymph were obtained by lymphatic duct cannulation.

Results. Unlike the solution, nanoparticles did concentrate AZT very efficiently in the intestinal mucosa, as well as in the Peyer's patches, and could simultaneously control the release of free AZT. Concentration in Peyer's patches was 4 times higher for nanoparticles, compared with the control solution. The tissue concentration was 30–45 μM, which was much higher than the reported IC_{50} of AZT (0.06–1.36 μM) and was regularly distributed along the gastrointestinal tract.

Conclusions. Nanoparticles have been shown to be efficient in concentrating AZT in the intestinal epithelium and gut-associated lymphoid tissues, supporting the view that these particles may represent a promising carrier to treat specifically the GI reservoir of HIV.

KEY WORDS: poly(isohexylcyanoacrylate) nanoparticles; 3′-azido 3′-deoxythymidine (AZT); intestinal epithelium; lymphatic duct cannulation; Peyer's patches; gastrointestinal reservoir of HIV.

INTRODUCTION

Cells of the immune system play an important role in the AIDS pathogenesis. Lymphoid tissues act as a virus reservoir and a major replication site for human immunodeficiency virus (HIV). HIV infection is active and progressive in lymphoid tissues during the clinically latent stage of the disease (1). During early stages of the infection, viremia is relatively low and the number of infected cells in the blood is minimal while intense replication occurs in lymphoid tissues (2). The clinical phase corresponds to a sudden increase of the viremia. The gastrointestinal tract contains a high concentration of various immunocompetent cells (3), which are an important target for HIV. The presence of the virus has been identified in mononuclear cells of the lamina propria (lymphocytes, macrophages) (4), and also in M-cells (5). Moreover, the presence of HIV in enterocytes has also been suspected by Heise *et al.* (6). The localization of the virus at these levels has at least two major consequences. First, HIV is active in the gut-associated lymphoid tissues (GALT) throughout the period of clinical latency, although at these times only minimal viral burden is observed in the blood (7). Secondly, it has been clearly established that pathologic effects such as chronic diarrhea were also associated to the presence of HIV in the mucosal tissue (4). Therefore, the intestinal tissue constitute a HIV reservoir which should be specifically addressed.

AZT is a powerful inhibitor of reverse transcriptase. It is a water-soluble drug characterised by a short half-life (1.1 hours) (8), meaning that substantial localization in the gastrointestinal tract cannot be obtained by conventional dosage forms. Therefore, the aim of the present study was to concentrate AZT into or close to these target cells. Poly(isohexylcyanoacrylate) nanospheres were selected as drug carriers because of their adequate controlled release characteristics in the gastrointestinal tract, as well as their tendency to interact with the intestinal mucosa (9).

MATERIALS AND METHODS

Chemicals

Isohexylcyanoacrylate was donated by Loctite (Ireland). AZT and dextran 70,000 were purchased from Sigma (France). Radiolabeled ^{3}H AZT and sodium dioctylsulfosuccinate were purchased from Isotopchim (France) and Fluka (France), respectively. Pepsin from porcine stomach mucosa and pancreatin from porcine pancreas were obtained from Sigma (France). Other reagents were analytical grade.

Nanoparticles Preparation

Poly(isohexylcyanoacrylate) nanoparticles were prepared according to a manufacturing process derived from Löbenberg *et al.* (10). Briefly, 50 μl of monomer were added to 5 ml of an acidic medium (HCl 0.01 M) containing 8.3 mg of sodium dioctylsulfosuccinate and 12.5 mg of dextran. Five milligrams of AZT and 30 μCi of ^{3}H-AZT for radiolabeling the particles were also added. After 96 hours under magnetic stirring (600 rpm), the particles were filtered (Millex AP 500, Millipore, France) and centrifuged at 7,590 g for 30 minutes to eliminate unbound AZT before administration.

Characterization of the Nanospheres

AZT loading was analyzed by liquid scintillation in a scintillation counter (LS 6000 TA counter, Beckman, France) after centrifugation of the colloidal suspension at 7,590 g for 30 minutes. The content in AZT was calculated simultaneously in the pellet and the supernatant. These amounts were compared to the total weight of the particles in the suspension, which was determined after freeze drying a non-radiolabeled suspension prepared under similar conditions. The AZT loading, expressed as a percentage of the particle

[1] UMR 8612, Université de Paris XI, 5, rue J.B. Clément, 92296 Châtenay-Malabry, France.

[2] To whom correspondence should be addressed. (e-mail: gilles.ponchel@cep.u-psud.fr)

0724-8741/01/0400-0467$19.50/0

weight, was around 8% and the yield of encapsulation was approximately 50%.

Particle Size and Zeta Potential

Particle size was measured by laser light scattering (Nanosizer ND4, Coultronics, France). The average diameter of the particles was 250 ± 20 nm. The zeta potential of the particles was −23 ± 5 mV as determined by doppler laser velocimetry in NaCl 10^{-3} M (Malvern Zetasizer®, Malvern Instruments, UK).

In Vitro Release Experiments

In vitro release of AZT from the nanoparticles was estimated in triplicate in distilled water and in USP XXIII simulated gastric and intestinal media. 0.2 mg/ml of radiolabeled particles was placed in the media at 37°C for 8 hours. Samples were placed in Ultrafree tubes with a cutoff of 30,000 Da (Ultrafree, MC Millipore, Bedford, USA) and centrifuged for 5 min at 7,590 g. Finally, amounts of AZT in the ultrafiltrates were determined by liquid scintillation after being mixed with 10 ml of Hionic Fluor®. Adsorption on the filters was negligible.

Animal Experiments

Determination of AZT Concentration in the Intestine

Before experimentation, Wistar rats (175–200 g, Charles River, France) were kept in metabolic cages for 16 hours with free access to water only. For each experimental time (30 and 90 minutes), a suspension of radiolabeled AZT nanospheres was given to a group of three rats by intragastric intubation. Similarly, a control water solution of AZT was administered to two other groups of three rats. Each preparation (1 ml) was administered to the rats as a single dose of 0.25 mg AZT (1.4 μCi)/100 g of body weight. The animals were kept in individual cages after dosing.

Two milliliters of blood was taken from the portal vein. It was assumed that total blood volume was equivalent to 6.4% of the body weight. Urine as well as the liver, lungs, spleen and gastrointestinal tract were simultaneously removed.

To evaluate the particles interaction with the mucosa, the intestine was cut into 5-cm segments. The segments were washed with physiological saline (NaCl, 0.9% [w/v]) to eliminate non adhering particles. The mucus was gently scraped with a spatula and any visible Peyer's patch was carefully dissected.

Intestine, mucus, and epithelium were weighed and digested in 1 ml of Soluene-350® at 50°C overnight, and further 10 ml of a scintillation cocktail (Hionic Fluor®, Packard, France) was added. Stomach, colon, and caecum were cut into three equal pieces and dissolved in 2 ml of Soluene-350®. Radioactivity in urine samples was directly counted after being mixed with a scintillation cocktail (Ultima-Gold, Packard, France). Blood samples were treated as follows: 100 μl of blood was mixed with 1 ml of a Soluene-350®/Isopropanol (1/1) mixture. Then, 0.4–0.5 ml of 30% H_2O_2 solution was added dropwise and 10 ml of scintillation cocktail was added before counting.

For other organs, two samples of 60 mg of each organ were dissolved in 1 ml of Soluene-350® at 50°C overnight. The samples showing intense coloration were lightened with 200 μl of 30% H_2O_2 solution and finally counted in a liquid scintillation counter.

For each experimental point (preparation and time), the mean of three replicates was calculated.

Mesenteric Duct Cannulation

To detect lymphatics, a second group of rats were dosed with 1 ml of oleic acid. They were kept in metabolic cages for 90 minutes to allow oil digestion. Then, they were anesthetized by intraperitoneal administration of pentobarbital (6 mg/kg of body weight). The mesenteric lymph duct was cannulated by a procedure described by Warshaw (11). Briefly, a cannula (external and internal diameter were 0.7 and 0.61 mm, respectively) was introduced into the major mesenteric lymph duct. The cannula was kept in place with a drop of instant bioadhesive glue (Dermabond, Ethicon, Sommerville, USA). Two hours after surgery, the rats having recovered consciousness, were given either the nanospheres or the control solution by oral gavage. Lymph samples were collected at 30, 60, 90, 120, 180, and 240 minutes, and the radioactivity was evaluated. Before counting, lymph samples were weighed and digested in 1 ml of Soluene-350®.

RESULTS

In a preliminary study, we investigated the behavior of nanoparticles in several media in order to verify that AZT could be released from nanoparticles. Figure 1 shows the release profiles of AZT from nanoparticles in different media. Release was strongly dependant upon the presence of esterases in the release medium. In water or in the USP XIII-simulated gastric medium containing pepsin, a burst release of 35% AZT was observed followed by a prolonged plateau (40% released after 8 hours). In the pancreatin-supplemented medium, the AZT release was more progressive and reached almost 80% after 8 hours, which could possibly be attributed to the progressive enzymatic degradation of the polymer by esterases contained in pancreatin.

AZT was administered to the rats as a colloidal suspension of nanoparticles and a control solution, respectively. Results were expressed in terms of AZT concentrations in the different organs (except for Fig. 2), as they were considered to be more relevant than absolute doses.

Interestingly, because of their specific affinity for the intestinal mucosa, poly(isohexylcyanoacrylate) nanospheres were able to concentrate at least 4.4 and 5.9 times more AZT in the gastrointestinal tract when compared to the control solution after 30 and 90 min., respectively (Fig. 2). This difference was rapidly noticeable as early as 30 minutes after administration and lasted for at least 1 hour. When associated to nanospheres, 67 and 64% of the initial dose of AZT was found in the gastrointestinal tract after 30 and 90 minutes, respectively, whereas when given in the form of a solution, it amounted to 15 and 11% only, respectively. The data relative to the AZT solution suggested that an important fraction of AZT was absorbed and eliminated by urinary excretion as soon as 30 minutes after dosing. Conversely, nanospheres ensured a prolonged localization of AZT in the gastrointestinal tract, corresponding to an incomplete systemic absorption of

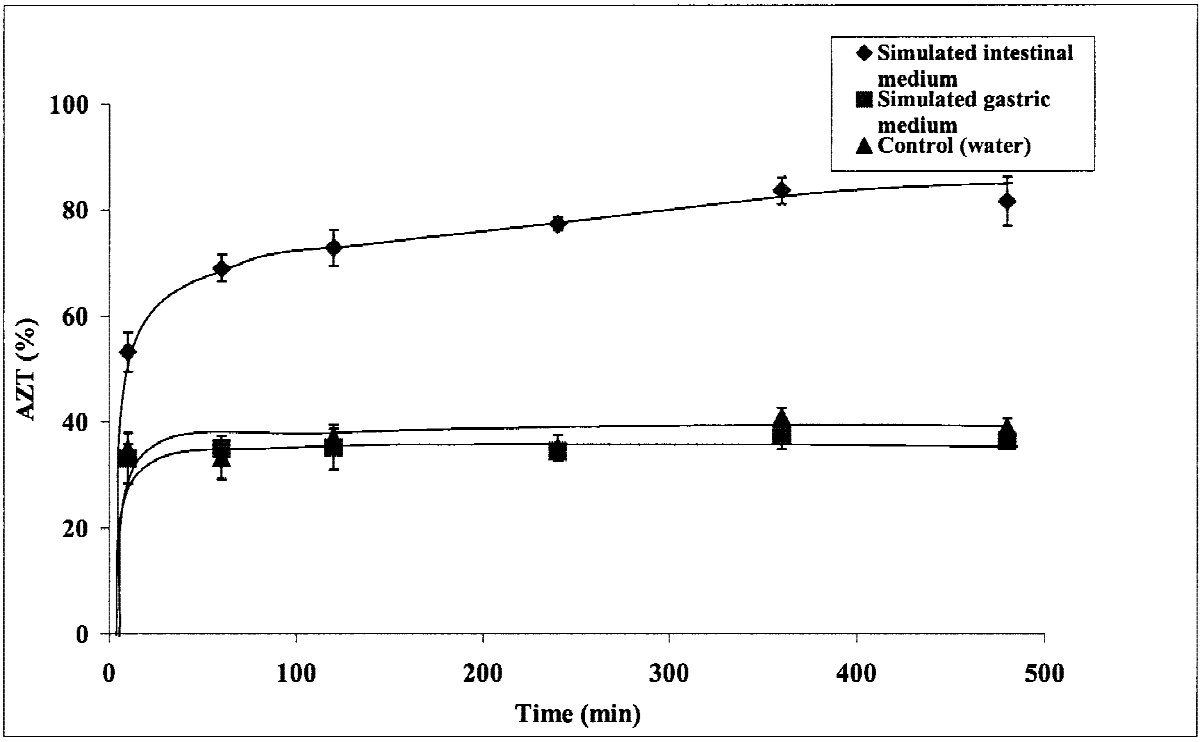

Fig. 1. Release kinetics of AZT from nanospheres in various media (n = 3). Bars represent standard deviations.

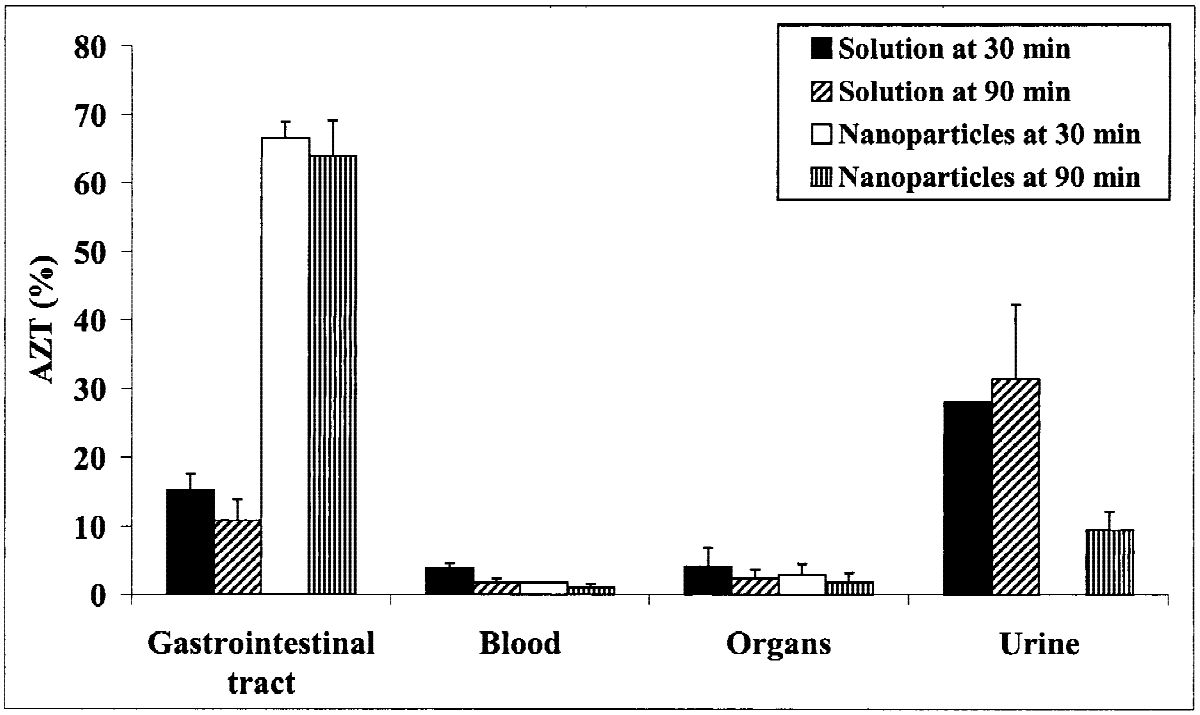

Fig. 2. Distribution of AZT in the body. Dose = 0.25 mg AZT/100 g of body weight, means of three replicates. Liver, spleen, lungs, and kidneys are gathered together under the term "organ." Bars represent standard deviations.

AZT at this early time. Comparatively, AZT concentrations in the blood and in other organs (including liver, spleen, kidneys and lungs, data not shown) were quite low, for both the solution and the nanospheres.

Radioactivity was distributed between the gastrointestinal tissue and the luminal contents (data not shown). Figure 3 shows the distribution of AZT in the gastrointestinal tissue. Concentrations in the stomach and intestine were high when compared with the caecum and colon. Considering the concentrations associated to the mucosa (epithelium and mucus), the difference between the two formulations was large (Fig. 3A). In the case of particles, AZT concentrations in the stom-

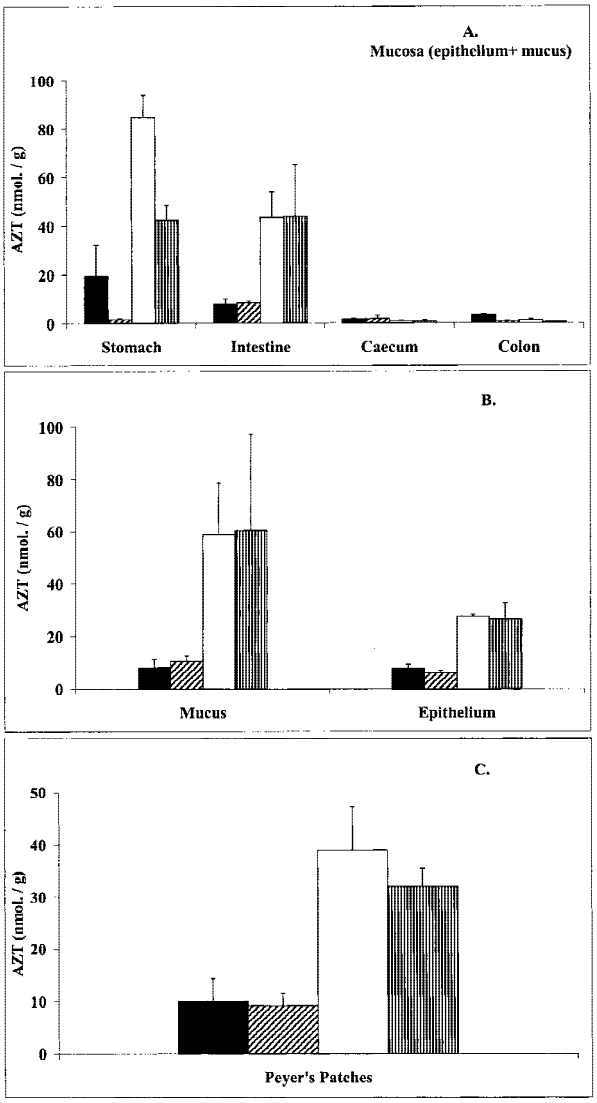

Fig. 3. Detailed distribution of AZT in the gastrointestinal tract and other organs at 30 and 90 minutes. Dose = 0.25 mg AZT/100 g of body weight, means of three replicates. (A) Distribution of AZT concentrations in the gastrointestinal tract; (B) AZT concentration in the mucus and epithelium; (C) AZT concentration in Peyer's patches for solution at 30 and 90 minutes (■, ▨) and the nanoparticles at 30 and 90 minutes (□, ▥) respectively. Bars represent standard deviations.

ach were 4 and 28 folds higher than the solution after 30 and 90 min, respectively, whereas it was 5.5 and 5.3 folds greater in the intestine after the same time points, respectively. The particles could also maintain constant high concentrations of AZT in the intestine (43.6 and 43.9 nmol. of AZT/g of organ after 30 and 90 min, respectively). Concentrations in the caecum and colon were still low and comparable for both formulations, probably resulting from slow transit up to 90 minutes.

When expressed in terms of absolute doses, the amounts of AZT associated to the intestinal mucosa were much higher than those in the stomach. AZT amounts recovered in the stomach, expressed as percentages of the initial dose, were 1.9% and 0.15% for the solution and 8.3% and 4.2% for the particles, after 30 and 90 minutes, respectively. In the intestine (epithelium + mucus), the amounts expressed as a percentage of the initial dose were 3.9% and 4.1% for the solution and 21.4% and 21.5% for the nanoparticles at the same time points, respectively.

In the epithelium, concentrations of AZT were much higher for the nanoparticles than for the solution (27.4 and 26.4 nmol/g of organ for nanoparticles and 7.8 and 5.9 nmol/g of organ for the solution at 30 and 90 minutes, respectively). Moreover, for nanoparticles, the concentration present in the mucus layer was at least three times as high as the one measured in the epithelium (Fig. 3B).

Additionally, nanoparticles resulted in much higher AZT concentrations in the mucus when compared to the solution (59.0 and 60.5 nmol. of AZT/ g of organ for the nanoparticles at 30 and 90 minutes, respectively, compared with 8.1 and 10.6 nmol/g of organ for the solution).

Finally, nanoparticles concentrated efficiently AZT in the Peyer's patches (Fig. 3C) where AZT concentrations were in the range of 30–45 nmol AZT/g of organ for nanoparticles and 4-fold greater than for the solution.

The detailed distribution of AZT along the gastrointestinal tract is presented in Fig. 4. As early as 30 minutes after administration, high concentrations of AZT were observed both in the mucosa and the mucus along the whole length of the small intestine in the case of the nanospheres, indicating a rapid transit of the nanoparticles. Associated amounts of AZT were evenly distributed between the epithelium and the mucus. Ninety minutes after administration, AZT could be

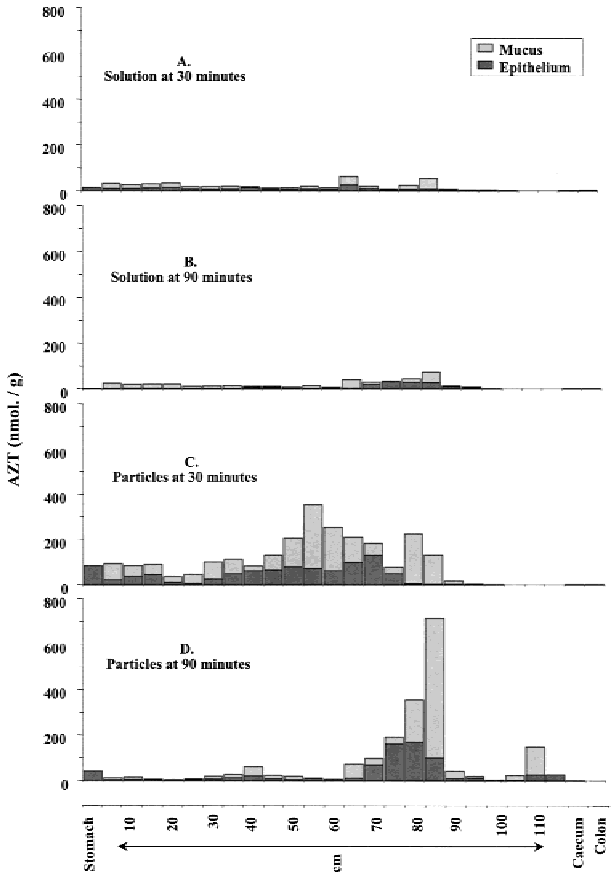

Fig. 4. Spacial distribution of AZT along the gastrointestinal tract (n = 3). Bars represent standard deviations.

detected along the whole gut with a maximal concentration in the distal intestine, resulting from particle transit and progressive mucus renewal. In the case of the solution, only low concentrations of AZT were associated to the epithelium and the mucus. Radioactivity was negligible in colon and caecum at these times.

We further considered if the association of AZT to nanospheres could increase the presence of the drug in the lymphatics. For both formulations, AZT concentration was maximal after 60 minutes in the lymph and in the Peyer's patches and then decreased with time (Fig. 5). The lymph concentrations were approximately 4- to 10-fold higher for the AZT solution. Nevertheless, association of AZT to the nanoparticles allowed a 4-fold increase in the AZT concentration in the Peyer's patches. As shown from the calculation of the ratio of the concentrations between AZT in the Peyer's patches and in the lymph, nanoparticles concentrated AZT very efficiently in the Peyer's patches. This ratio for the solution was only 4- and 3-fold after 30 and 90 minutes, respectively, indicating a moderate affinity of AZT for these cells, whereas for nanoparticles the ratio was 72 and 34 times at 30 and 90 minutes, respectively. It suggested that an efficient uptake of the particles by the M cells of Peyer's patches had occurred, which minimised the amount of free AZT reaching the lymphatic flow.

DISCUSSION

T-lymphocytes, macrophages (4,5), and also possibly follicular dendritic cells (12), play an important role in HIV infection and immunopathogenesis of AIDS. These cells act as a reservoir for the HIV and are believed to be responsible for its dissemination throughout the body. The ability of antiviral drugs to access these cells in sufficient concentration is therefore critical to the success of AIDS therapy.

The gastrointestinal tract has the largest amount of immune cells in the body and an important fraction of the viral burden is located in these cells. Major consequences result from this situation. In the initial period of clinical latency, HIV could be still detected in intestinal biopsies while it was undetectable in peripheral blood (7). It has been shown that the loss of $CD4^+$ lymphocytes in the duodenum of infected patients was more pronounced than in the peripheral blood (7), resulting in the decrease of the efficiency of the intestinal barrier against pathogens. Furthermore, HIV can be detected in the intestinal tract of 30–75% of HIV-positive patients with intestinal symptoms and may be responsible for chronic diarrhea manifestations (13).

Therefore, a possible strategy may consist, in addition to a systemic medication, of specifically treating this major reservoir of virus by targeting the intestinal tissue. For this purpose, nanospheres are promising drug delivery systems for the following reasons: (i) because of their small size and high specific surface they can interact very efficiently with the intestinal mucosa, (ii) because to some extent they can be internalized by cells, and (iii) because drug release can be time controlled.

After oral administration, there is some evidence in the present work that poly(isohexylcyanoacrylate) particles were captured efficiently by the mucosa, as indicated by the general increase in AZT concentration in the epithelium itself as well as in the mucus layer. Different mechanisms can be responsible for such a capture. First, it has been shown by Durrer *et al.* (14), that the glycoproteic gel constituting the mucus acted as a porous adsorbent in which small nanospheres can diffuse

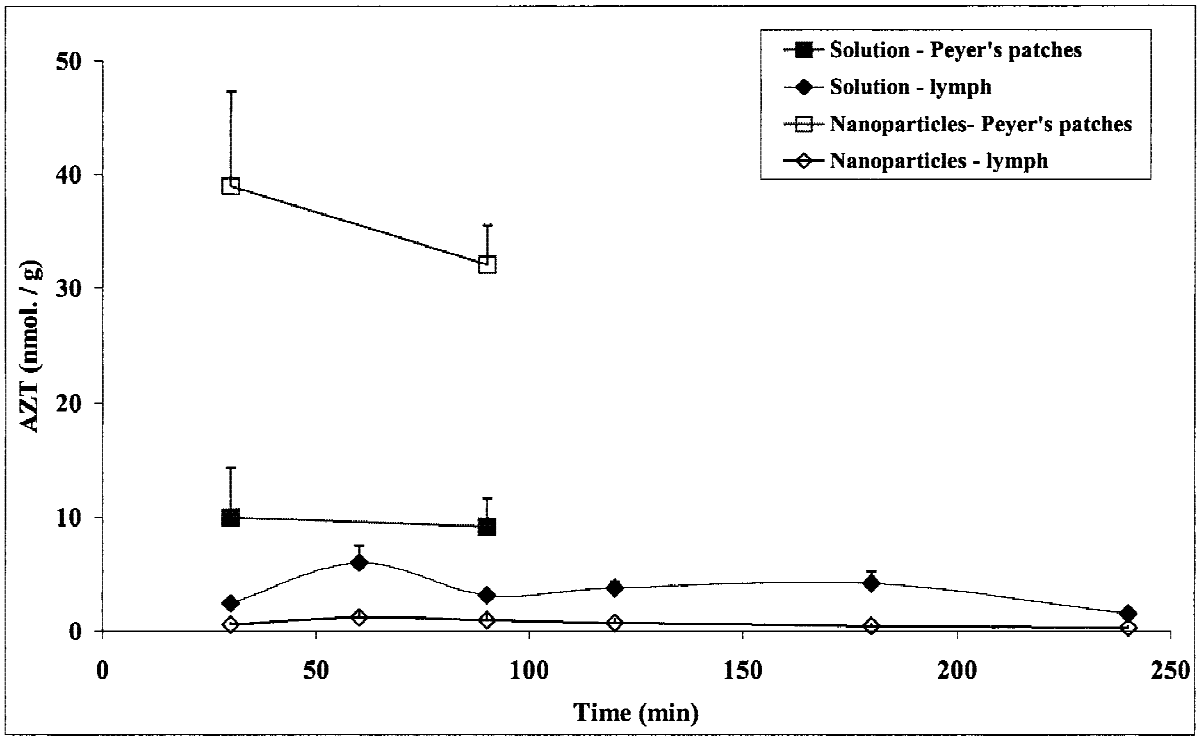

Fig. 5. Concentration of AZT in lymph compared with the concentration in the Peyer's patches (n = 3). Bars represent standard deviations.

and be immobilised until mucus renewal. Poly(isobutylcyanoacrylate) nanospheres have been shown to have the same behavior (9). Second, particle uptake has been reported to occur to some extent not only in Caco-2 cell cultures (15) but also in the mucosa (16), the M cells (17) of Peyer's patches, and even in the lymphatics (18). However, particle uptake is generally a rather slow process (19), whereas particle adhesion to the mucosa is a fast and quantitatively much more important phenomenon (9). In turn, because of immobilization, an increase in the contact time would result in an enhanced uptake.

In this regard, the detailed distribution of encapsulated AZT at different intestinal levels resulted from these different mechanisms. The nanoparticles formed a regular deposit of AZT along the intestine. Compared with the control solution, AZT bound to nanoparticles was concentrated not only in the mucus layer but also in the epithelium itself. Increase in AZT concentrations in the Peyer's patches could be related to particle uptake by M cells. It was observed that AZT affinity for these cells was dramatically increased by encapsulation, which resulted in a minimisation of AZT loss in the circulating lymph. After endocytosis, migration of drug loaded immunocompetent cells to the lymph nodes can therefore be expected.

AZT was selected in the present study because it remains the most important drug in AIDS-therapy. It is usually given in combination with other nucleosidic analogs and/or antiproteases to reduce drug resistance, minimise toxicity and side effects. However, bone marrow toxicity, haematological changes and short elimination half-life ($t_{1/2}$ = 1.1 hour) (8) limit the AZT effectiveness. Encapsulation in different carrier systems, as liposomes (20) or rescelled erythrocytes used as drug carriers (21) have shown beneficial effects on drug delivery and minimised side effects of AZT.

Löbenberg *et al.* (22) deducted from plasmatic profiles that oral administration of AZT associated to poly(isohexylcyanoacrylate) nanoparticles resulted in a delayed absorption of the drug. This behaviour was attributed to a possible bioadhesion phenomenon in the GI-tract. In the present study, we investigated the potential of poly(isohexylcyanoacrylate) nanoparticles to target and to concentrate AZT in the digestive tissue. Interestingly our work confirmed the existence of an intimate interaction between nanoparticles and the gastrointestinal mucosa. Nanoparticles behaved as a prolonged release dosage form and resulted in the accumulation of AZT in the intestinal tissue. As suggested in Figure 1, it is likely that the amounts of drug measured in the intestine at the early experimental times adopted in the study represented not only free drug but also drug bound to the nanoparticles in a proportion which remains unknown *in vivo*. However, once localised in the mucus or the intestinal tissue, release studies showed that AZT could be totally released by the enzymatic action of esterases, as described previously for poly(isohexylcyanoacrylate) nanoparticles, within a period of time compatible with oral delivery. This release probably corresponds to a complete degradation of the nanospheres (23). Finally, an earlier study on the present formulation confirmed that AZT bound to poly(isohexylcyanoacrylate) nanospheres retained their anti-viral activity (24), and moreover, cell culture experiments demonstrated that chronic HIV infection of macrophages resulted in enhanced phagocytic activity against these particles compared to non infected cells (25).

The very low levels of AZT detected in the lymph after nanoparticle administration suggested that an efficient capture of the particles occurred through the Peyer's patches, resulting in an intracellular localization of the drug. As a result, it can be hypothesised that some immune cells will carry AZT to the mesenteric lymphatic nodules, where an important viral burden is located and which constitutes a major replication site of HIV (26). Finally, it should be underlined that complete release of free AZT from nanoparticles is expected in these cells due to particle esterase sensitivity.

Favorably, one of the finding of the present study is that the tissue concentrations in the intestinal mucosa and in the Peyer's patches were much higher than reported IC_{80} values for AZT. Reported IC_{50} values range between 0.06 and 1.36 μM, depending on the experimental conditions (27–30). For example, Aggarwal *et al.* (28), testing the antiviral activity of AZT on infected peripheral blood mononuclear cells (PBMC) from seronegative donors, reported an IC_{50} of 0.12 μM, whereas Daluge *et al.* reported an IC_{50} of 0.23 μM for AZT sensitivity on clinical isolates (30). In the present work, the tissue concentrations of AZT, which were likely to be generated after complete release of AZT from the nanoparticles in the epithelium and the Peyer's patches, were in the range of 30–45 μM (assuming that the density of tissues was close to 1). Such a comparison is only indicative because of the complexity of organs, which can lead to heterogeneous distributions compared with cell cultures. This result suggests, however, that nanoparticles are very promising tools for targeting AZT at effective antiviral concentrations to the gastrointestinal HIV reservoir.

CONCLUSION

Especially noteworthy for AIDS therapy is the finding that poly(isohexylcyanoacrylate) nanoparticles are able to target and concentrate AZT in the intestinal epithelium and the associated immunocompetent cells of the GALT. Therefore, in addition to a systemic treatment, nanoparticles can provide a promising means to specifically treat one of the major HIV reservoirs in the body. Very probably, this technique could be extended to other anti-HIV drugs.

ACKNOWLEDGMENTS

The Loctite company is fully acknowledged for their contribution.

REFERENCES

1. G. Pantaleo, C. Graziosi, J. F. Demarest, L. Butini, M. Montroni, C. H. Fox, J. M. Orenstein, D. P. Kotler, and A. S. Fauci. HIV infection is active and progressive in lymphoid tissue during the clinically latent stage of disease. *Nature* **362**:355–358 (1993).
2. J. Embretson, M. Zupancic, J. L. Ribas, A. Burke, P. Racz, K. Tenner-Racz, and A. T. Haase. Massive covert infection of helper T lymphocytes and macrophages by HIV during the incubation period of AIDS. *Nature* **362**:359–362 (1993).
3. H. B. Mayer and C. A. Wanke. Diagnostic strategies in HIV-infected patients with diarrhea. *Aids* **8**:1639–1648 (1994).
4. J. A. Nelson, C. A. Wiley, C. Reynolds–Kohler, C. E. Reese, W. Margaretten, and J. A. Levy. Human immunodeficiency virus detected in bowel epithelium from patients with gastrointestinal symptoms. *Lancet* **1**:259–262 (1988).
5. M. R. Neutra. Interactions of viruses and microparticles with apical plasma membranes of M cells: Implications for human im-

munodeficiency virus transmission. *J. Infect. Dis*. **179**:S441–443 (1999).
6. C. Heise, S. Dandekar, P. Kumar, R. Duplantier, R. M. Donovan, and C. H. Halsted. Human immunodeficiency virus infection of enterocytes and mononuclear cells in human jejunal mucosa. *Gastroenterology* **100**:1521–1527 (1991).
7. T. Schneider, H. U. Jahn, W. Schmidt, E. O. Riecken, M. Zeitz, and R. Ullrich. Loss of CD4 T lymphocytes in patients infected with human immunodeficiency virus type 1 is more pronounced in the duodenal mucosa than in the peripheral blood. Berlin Diarrhea/Wasting Syndrome Study Group. *Gut* **37**:524–529 (1995).
8. X. Li and W. K. Chan. Transport, metabolism and elimination mechanisms of anti-HIV agents. *Adv. Drug Deliv. Rev*. **39**:81–103 (1999).
9. G. Ponchel, M.-J. Montisci, A. Dembri, C. Durrer, and D. Duchêne. Mucoadhesion of colloidal particulate systems in gastrointestinal tract. *Eur. J. Pharm. Biopharm.* **44**:25–31 (1997).
10. R. Löbenberg, L. Araujo, H. von Briesen, E. Rodgers, and J. Kreuter. Body distribution of azidothymidine bound to hexylcyanoacrylate nanoparticles after i.v. injection to rats. *J. Control. Release* **50**:21–30 (1998).
11. A. L. Warshaw. A simplified method of cannulating the intestinal lymphatics of the rat. *Gut* **13**:66–67 (1972).
12. A. T. Haase, K. Henry, M. Zupancic, G. Sedgewick, R. A. Faust, H. Melroe, W. Cavert, K. Gebhard, K. Staskus, Z. Q. Zhang, P. J. Dailey, H. H. J. Balfour, A. Erice, and A. S. Perelson. Quantitative image analysis of HIV-1 infection in lymphoid tissue. *Science* **274**:985–989 (1996).
13. J. J. Mathewson, Z. D. Jiang, H. L. DuPont, C. Chintu, N. Luo, and A. Zumla. Intestinal secretory IgA immune response against human immunodeficiency virus among infected patients with acute and chronic diarrhea. *J. Infect. Dis.* **169**:614–617 (1994).
14. C. Durrer, J. M. Irache, F. Puisieux, D. Duchêne and G. Ponchel. Mucoadhesion of latexes. II. Adsorption isotherms and desorption studies. *Pharm. Res.* **11**:680–683 (1994).
15. M. P. Desai, V. Labhasetwar, E. Walter, R. J. Levy, and G. L. Amidon. The mechanism of uptake of biodegradable microparticles in Caco-2 cells is size dependent. *Pharm. Res.* **14**:1568–1573 (1997).
16. G. M. Hodges, E. A. Carr, R. A. Hazzard, and K. E. Carr. Uptake and translocation of microparticles in small intestine. Morphology and quantification of particle distribution. *Dig. Dis. Sci.* **40**: 967–975 (1995).
17. M. W. Smith, N. W. Thomas, P. G. Jenkins, N. G. Miller, D. Cremaschi, and C. Porta. Selective transport of microparticles across Peyer's patch follicle-associated M cells from mice and rats. *Exp. Physiol.* **80**:735–743 (1995).
18. P. G. Jenkins, K. A. Howard, N. W. Blackhall, N. W. Thomas, S. S. Davis, and D. T. O'Hagan. The quantitation of the absorption of microparticles into the intestinal lymph of Wistar rats. *Int. J. Pharm.* **102**:261–266 (1994).
19. D. T. O'Hagan. The intestinal uptake of particles and the implications for drug and antigen delivery. *J. Anat.* **189**:477–482 (1996).
20. N. C. Phillips and C. Tsoukas. Liposomal encapsulation of azidothymidine results in decreased hematopoietic toxicity and enhanced activity against murine acquired immunodeficiency syndrome. *Blood* **79**:1137–1143 (1992).
21. U. Benatti, M. Giovine, G. Damonte, A. Gasparini, S. Scarfi, A. De Flora, A. Fraternale, L. Rossi, and M. Magnani. Azidothymidine homodinucleotide-loaded erythrocytes and bioreactors for slow delivery of the antiretroviral drug azidothymidine. *Biochem. Biophys. Res. Commun.* **220**:20–25 (1996).
22. R. Löbenberg, L. Araujo, and J. Kreuter. Body distribution of azidothymidine bound to nanoparticles after oral administration. *Eur. J. Pharm. Biopharm.* **44**:127–132 (1997).
23. D. Scherer, J. R. Robinson, and J. Kreuter. Influence of enzymes on the stability of polybutylcyanoacrylate nanoparticles. *Int. J. Pharm.* **101**:165–168 (1994).
24. A. Bender, V. Schäfer, A. M. Steffan, C. Royer, J. Kreuter, H. Rubsamen-Waigmann, and H. von Briesen. Inhibition of HIV in vitro by antiviral drug-targeting using nanoparticles. *Res. Virol.* **145**:215–220 (1994).
25. V. Schäfer, H. von Briesen, R. Andreesen, A. M. Steffan, C. Royer, S. Troster, J. Kreuter, and H. Rubsamen-Waigmann. Phagocytosis of nanoparticles by human immunodeficiency virus (HIV)-infected macrophages: A possibility for antiviral drug targeting. *Pharm. Res.* **9**:541–546 (1992).
26. G. Pantaleo, C. Graziosi, L. Butini, P. A. Pizzo, S. M. Schnittman, D. P. Kotler, and A. S. Fauci. Lymphoid organs function as major reservoirs for human immunodeficiency virus. *Proc. Natl. Acad. Sci. USA* **88**:9838–9842 (1991).
27. P. Herdewijn, J. Balzarini, E. De Clercq, R. Pauwels, M. Baba, S. Broder, and H. Vanderhaeghe. 3′-substituted 2′,3′-dideoxynucleoside analogues as potential anti-HIV (HTLV-III/LAV) agents. *J. Med. Chem.* **30**:1270–1278 (1987).
28. S. K. Aggarwal, S. R. Gogu, S. R. Rangan, and K. C. Agrawal. Synthesis and biological evaluation of prodrugs of zidovudine. *J. Med. Chem.* **33**:1505–1510 (1990).
29. B. A. Larder, S. D. Kemp, and P. R. Harrigan. Potential mechanism for sustained antiretroviral efficacy of AZT-3TC combination therapy. *Science* **269**:696–699 (1995).
30. S. M. Daluge, S. S. Good, M. B. Faletto, W. H. Miller, M. H. St. Clair, L. R. Boone, M. Tisdale, N. R. Parry, J. E. Reardon, R. E. Dornsife, D. R. Averett, and T. A. Krenitsky. 1592U89, a novel carbocyclic nucleoside analog with potent, selective anti-human immunodeficiency virus activity. *Antimicrob. Agents. Chemother.* **41**:1082–1093 (1997).